DOE Award # DE- SC0018962

Quantifying the Role of APB Tubes on the Work-hardening of Ordered Phases

P.I.: Ian Baker

Thayer School of Engineering, Dartmouth College, Hanover, New Hampshire, 03755

Ian.Baker@Dartmouth.edu

Report submitted: April 8th, 2022

Funding Period: August 1st, 2018-December 31st, 2021

Goal

For 60 years, it has been theorized that antiphase boundary (APB) tubes cause, or at least greatly contribute to, the high work hardening rate (WHR) of ordered intermetallic alloys. The initial aim of this work was to quantify that effect and directly link APB tube density to the WHR; however, as experiments were performed to that end, evidence mounted that APB tubes have no detectable effect on the WHR. Thus, the goal of this work shifted to rigorously confirming that APB tubes do not affect the WHR in FeAl and Ni_3Al and then observing Ni_3Fe to determine what is affecting the WHR. A number of high entropy alloys (HEAs) were screened but none were suitable for this work. They are discussed briefly in Appendix 1.

The concept of an APB tube was originally proposed by Vidoz and Brown [1] in 1962 to explain the much greater (~50% increase) WHR observed when an alloy, such as Ni_3Fe, is ordered. The existence of APB tubes was only definitively confirmed by Chou and Hirsch in 1981 [2] using weak-beam imaging with superlattice reflections in a transmission electron microscope. The most promising approach to how APB tubes can affect the strength of a material was put forth by Hazzledine and Sun in 1992 [3], including:

(i) by drag on primary edge dislocations,
(ii) by changing the cross-slip probability of primary screw dislocations,
(iii) by interacting with the stress fields of secondary coplanar dislocations,
(iv) and by acting as a forest to other secondary dislocations.

There has been no experimental evidence to prove or disprove any of these phenomena.

The main finding of this project is that antiphase boundary tubes do not contribute to the work hardening in FeAl or in Ni_3Al. instead, APB tubes should be considered as evidence of the complex superdislocation interactions that do give rise to the high WHR. Based on TEM *in-situ* straining of disordered and ordered Ni_3Fe, superdislocations in the ordered alloy were observed to undergo many more interaction events than unit dislocations in the disordered alloy, which can explain the increase in the WHR observed with ordering.

In this project, we addressed three major unresolved issues in this field: *(1)* there have been no studies comparing the mechanical properties of intermetallics with and without APB tubes; *(2)* the annealing temperature of APB tubes is only known for very few alloys; *(3)* proposed strengthening mechanisms almost entirely rely on *post-mortem* transmission electron microscopy (TEM) observations; and *(4)* the APB tube formation mechanism in Ni_3Al is still debated. Additionally, resistivity, X-ray diffraction, and neutron diffraction were used to try to quantify the density of APB tubes. Resistivity measurements are a promising technique and are discussed briefly. X-ray and neutron diffraction were not successful and are discussed in Appendix 2.

Summary of Key Results

(1) The hardness of B2-ordered FeAl did not change when APB tubes (and no other defects) were removed, indicating that APB tubes do not interact with gliding dislocations.

(2) The temperature at which APB anneal out of Ni_3Al was determined for the first time. TEM *in-situ* heating revealed that APB tubes anneal out at ~532°C. The annihilation was rapid and diffusion-controlled.
(3) Comparing the annihilation temperature of APB tubes in Ni_3Al to past literature, there is no marked change in the hardness, YS, or WHR around the temperature where APB tubes annihilate, indicating that APB tubes do not affect the hardening of Ni_3Al.
(4) *In-situ* TEM straining of ordered and disordered Ni_3Fe was used to observe the movement of dislocations to see what is causing the increase in WHR if it is not APB tubes. In the disordered alloy, dislocations moved rapidly though the material with very few pile-ups forming. In the ordered alloy, dislocations were observed interacting with dislocations on different planes and many large pile-ups were observed, both of which would increase the WHR.
(5) Bulk tensile testing of ordered and disordered Ni_3Fe showed that the WHR of ordered Ni_3Fe remained ~33% higher than disordered Ni_3Fe when strained at 480°C, which is consistent with the increase in WHR originating from superdislocation interactions.
(6) Throughout this work, thousands of micrographs of Ni_3Al were compiled. These micrographs are compared to APB tube formation mechanisms proposed in the literature.
(7) Resistivity measurements on FeAl indicate that resistivity might work for measuring APB tube density.

Detailed Observations

(1) Effect of APB tubes on the hardness of FeAl

While it has long been argued that APB tubes account for the high WHR of ordered intermetallics, no study had determined the mechanical properties before and after APB tube removal. In the experiment presented below, we introduced APB tubes in an Fe-40 at.% Al single crystal, measured the hardness, then annealed out the APB tubes and remeasured the hardness.

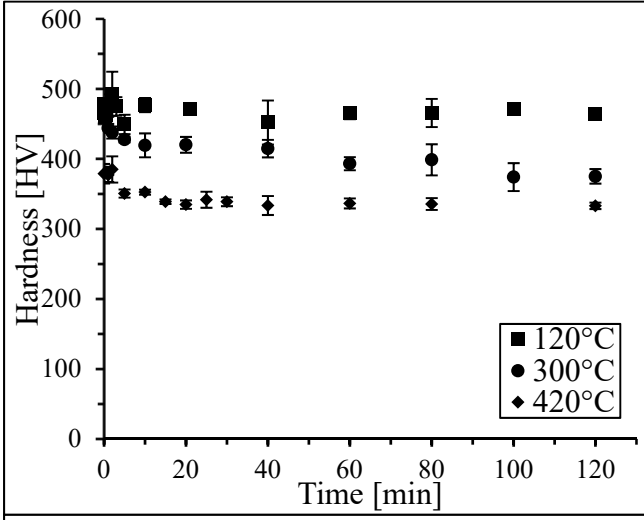

Figure 1. *Hardness of an Fe-40 at.% Al single crystal cold-rolled 16%, then annealed at the listed temperatures for up to 2 h.*

The hardness of an Fe-40 at.% Al single crystal was measured after 16% cold-rolling and annealing to remove APB tubes. **Figure 1** shows the hardness values after 16% cold-rolling and then annealing at various temperatures up to 2 h. The samples were annealed at *(i)* 120°C, the temperature at which the magnetic susceptibility drops dramatically [4–6], indicating APB tubes have annealed out; *(ii)* 300°C, near the onset of the second exothermic peak observed in DSC measurements [6]; and *(iii)* 420°C, near the third exothermic peak [6].

There was no decrease in hardness when annealing at 120°C, then a 19% decrease in hardness after annealing at 300°C for 2 h and an additional 9% drop after annealing at 420°C for 2 h. An Fe-43 at.% Al single crystal showed the same trend, but is not pictured here for brevity. It was surprising

that there was no change in hardness with annealing at 120°C. It is well established from magnetic testing [4–6] and direct observation [5] that APB tubes anneal out at this temperature, so it was anticipated that the hardness would decrease as well if APB tubes contribute to the strength by interacting with gliding dislocations. The softening at 300°C and 420°C are due to point defects and vacancies, respectively [7]. Thus, it is evident that APB tubes do not contribute to the hardening of FeAl by interacting with gliding dislocations.

(2) Annihilation of APB tubes in Ni_3Al

Lightly strained foils of Ni_3Al were heated *in-situ* in the TEM to determine the temperature at which APB tubes annihilate. APB tubes were readily visible as long highly rectilinear features and show up prominently with oscillating contrast when imaged with (111) reflections (for example, in **Figure 2a)**. Two heating experiments were performed. In the first test, shown in **Figure 2**, the APB tubes disappeared during a heating step from 507°C to 546°C. **Figure 2b** shows the same area of the foil after heating to 550°C and APB tubes are no longer visible. In the second test, the sample was held for ~10 min at 503°C, 520°C, 517°C, 525°C, 532°C, and 544°C. APB tubes were no longer visible after 6 minutes at 532°C. The disappearance of the APB tubes was rapid (~50 seconds when heating from 507°C to 546°C) and no changes in the foil were observed (e.g. the formation of a longitudinal kink along the tube as proposed by Ngan [8]) indicating the annihilation was diffusion-controlled.

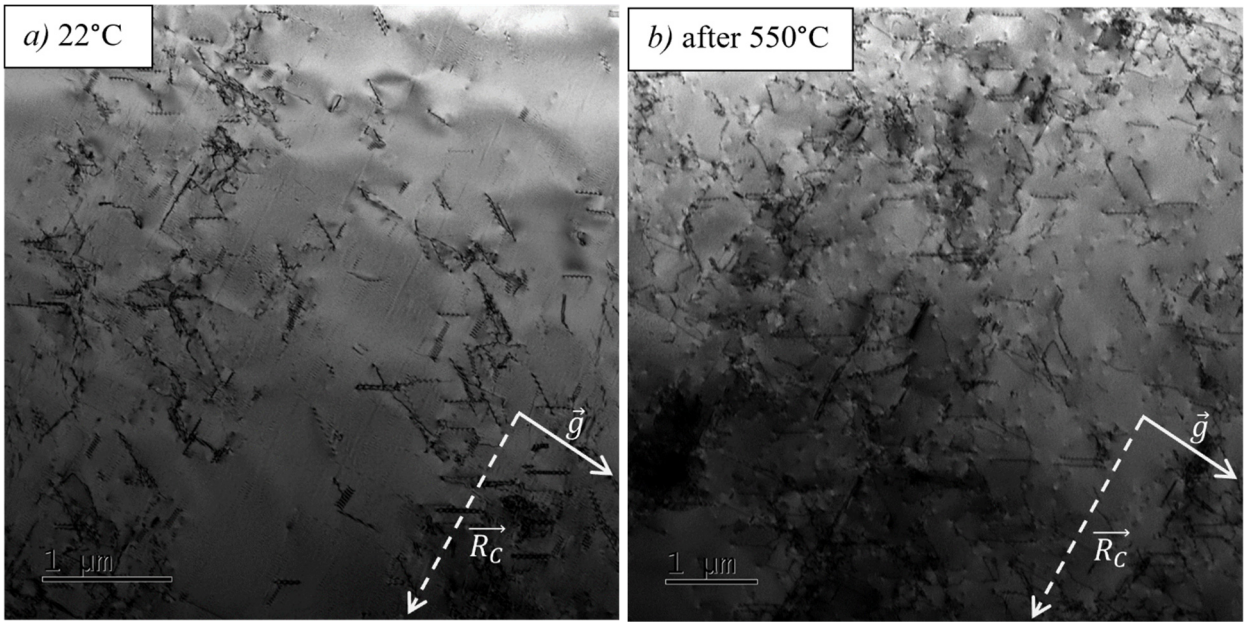

Figure 2. *Bright field TEM images of Ni_3Al compressed 1.9% a) at 22°C, and b) after heating to 550°C. Taken with $\vec{B} = [2\bar{3}5]$, $\vec{g} = [\bar{1}11]$, $\overrightarrow{R_C} = [110]$. Images are from roughly the same area of the sample.*

The annealing temperature of APB tubes in Ni_3Al is relatively high compared to that of Fe-40 at.% Al, which is 120°C [4–6]. This complicates matters, as other microstructural changes also occur with the removal of APB tubes. Near-edge dipoles collapsed into dislocation loops starting around 510°C. After heating, a decrease in the density of superlattice intrinsic stacking faults (SISF) observed. Thus, the hardness tests performed on FeAl could not be replicated in Ni_3Al, as other

defects would also annihilate out. Instead, the vast body of literature on the mechanical properties of Ni_3Al were reviewed and compared to the APB tube annihilation temperature.

Based on the theoretical strengthening proposed by Hazzledine and Hirsch [9] as well as Hazzledine and Sun [3] and using a shear modulus of 78 GPa [10] and {111} APB energy of 208 mJm^{-2} [11], the expected strengthening from APB tubes in Ni_3Al is ~10-70 MPa. This is a large portion of the total strength of Ni_3Al and should be noticeable if the strengthening decreases when APB tubes are removed. In hardness testing of deformed Ni_3Al, there is a continuous decrease in the hardness at temperatures above ~200°C but no abrupt decrease around 530°C, when the APB tubes would annihilate [12,13]. There also appears to be no effect on the yield strength (YS) or WHR of Ni_3Al when APB tubes are removed. Both have an anomalous positive temperature dependence. The YS increases steadily up to 700-800°C for all orientations [14–17] before declining. The WHR depends highly on the crystal orientation, but reaches a single or double peak then declines prior to 500°C for the orientations $[\bar{1}23]$ [15], $\langle 111 \rangle$, $\langle 001 \rangle$, $\langle 123 \rangle$, $\langle 144 \rangle$ [18], and ~$[\bar{3}68]$ [14]. APB tubes are not stable for the entire YS anomaly and persist slightly past the end of the WHR anomaly. Testing at temperatures where APB tubes annihilate leads to no noticeable drop in YS or WHR.

The trends observed in Ni_3Al were also observed in Ni_3Ga. Sun [30] reported that APB tubes were no longer observed in Ni_3Ga deformed at temperatures above 500°C. The WHR of single crystals of Ni_3Ga has a strong orientation dependence, but there is no marked change around 500°C when APB tubes are annihilated [121,122]. Additionally, it is well documented that APB tubes anneal out at 120°C in B2-ordered Fe-40 at.% Al [51,53]. The WHR measured at 1% strain for large-grained polycrystalline Fe-40 at.% Al strained at an initial strain rate of ~1 x 10-4 s-1 showed a slight decrease up to 227°C followed by a steep decline to zero at 477°C [109]. Thus, there is no experimental evidence that APB tubes have a large impact on the WHR of ordered intermetallics.

(3) Ni_3Fe tensile testing

If APB tubes do not contribute to the high WHR, what does? To answer this question, TEM *in-situ* straining was performed at room temperature on ordered and disordered Ni_3Fe. It was qualitatively evident that the dislocation motion during straining of disordered and ordered Ni_3Fe is very different. The unit dislocations in the disordered alloy moved smoothly and slipped out of the foil, with very few pile-ups observed. **Figure 3a** shows disordered Ni_3Fe at low strains, where the thick white arrow indicates an active dislocation source. **Figure 3b** shows the same area of the foil after greater strain, where a small pile-up was observed but most of the dislocations remained mobile.

The superdislocations in the ordered alloy moved far more jerkily than the unit dislocations in the disordered alloy. The superdislocations were observed locking and unlocking and getting pinned during cross-slip events. Octahedral cross-slip was very common, as shown in **Figure 3c**, which increases the chance of dislocation interactions. Most notably, large dislocation pile-ups were observed in the ordered alloy but not the disordered alloy. Pile-ups indicate that the leading dislocation has hit a barrier and more and more stress is required to overcome the barrier. The barrier in ordered Ni_3Fe appeared to be a tangle of cross-slipped screw superdislocations, as shown in **Figure 3d**. The high prevalence of superdislocation interactions in the ordered alloy could be the source of the high WHR.

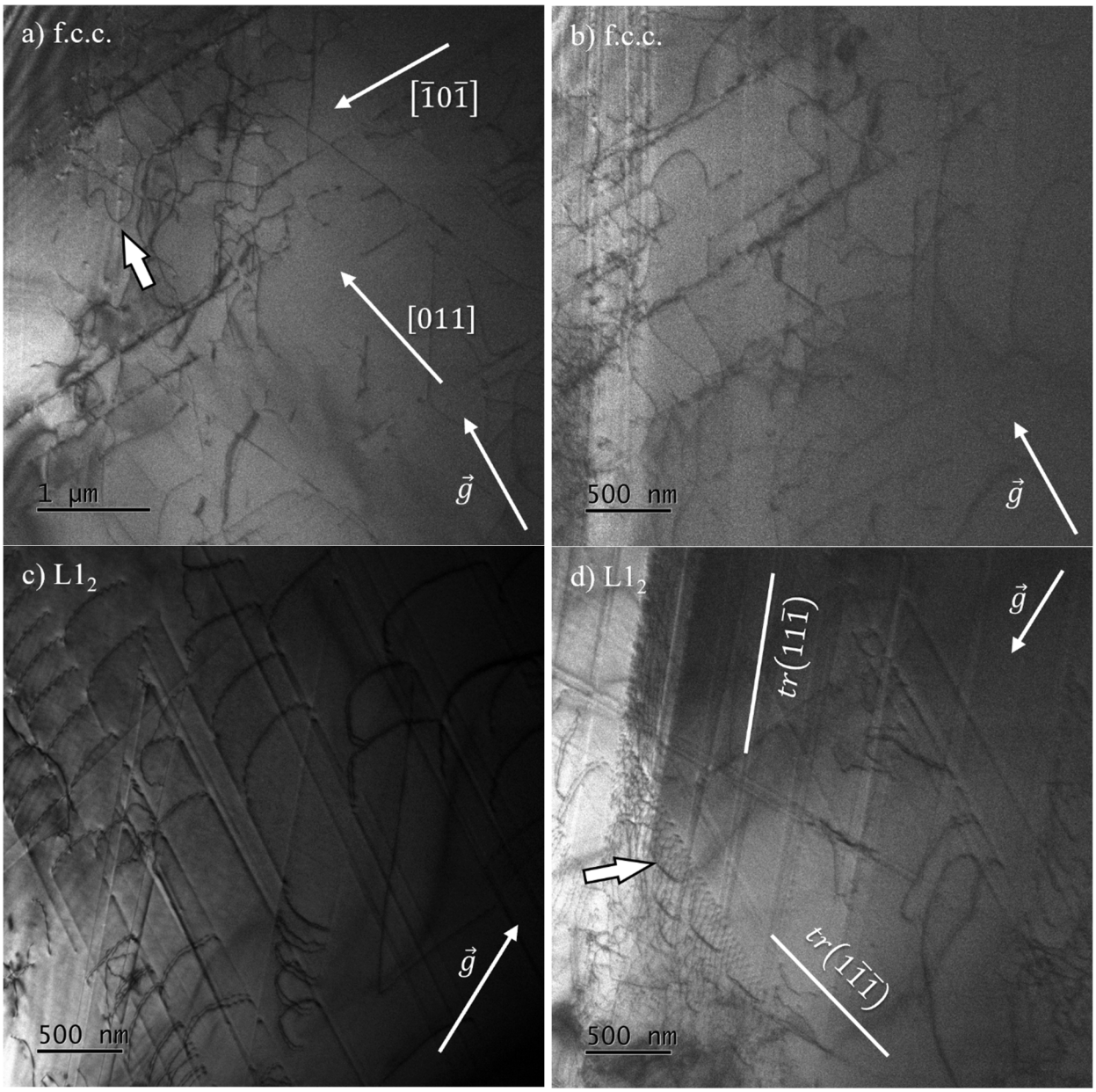

Figure 3. *Bright-field TEM images of dislocations during in-situ straining of a) disordered Ni_3Fe imaged with $\vec{B} = [110]$, $\vec{g} = [1\bar{1}\bar{1}]$; b) disordered Ni_3Fe imaged with $\vec{B} = [110]$, $\vec{g} = [1\bar{1}\bar{1}]$; c) ordered Ni_3Fe imaged with $\vec{B} = [5\bar{2}\bar{3}]$, $\vec{g} = [111]$; and d) ordered Ni_3Fe imaged with $\vec{B} = [7\bar{3}\bar{4}]$, $\vec{g} = [111]$. Solid white arrows indicate features of interest.*

A benefit of studying Ni_3Fe is that it is ductile enough to be strained in tension. Eight polycrystalline Ni_3Fe samples (all with the same texture) were strained in tension at an initial strain rate of 1 x 10^{-4} s^{-1}: one f.c.c. and one $L1_2$ sample were strained at room temperature, and three f.c.c. and three $L1_2$ samples were strained at 480°C (~0.97 T_c, where T_c is the order-disorder transition temperature [19]). All the tests are shown in **Figure 4**. Room temperature tensile tests were shown in a separate study to be highly repeatable (the YS and WHR of three samples from the same ingot had a standard deviation of 1%) and for the 480°C tests the WHR (measured at 275 MPa) had a standard deviation of 4%.

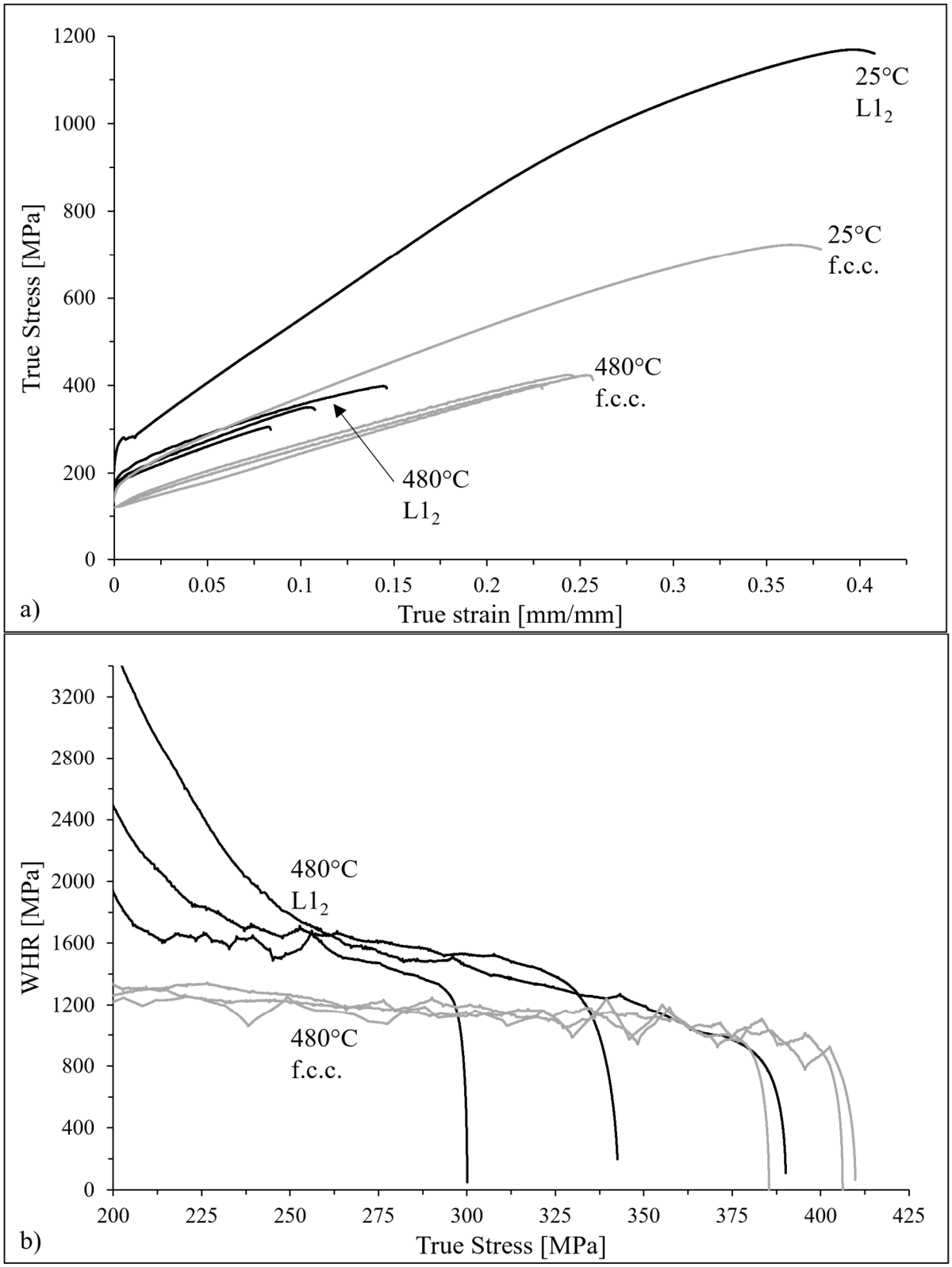

Figure 4. *Comparison of a) the true stress-strain and b) the WHR-stress curves of f.c.c. (grey) and $L1_2$ (black) Ni_3Fe strained at an initial strain rate of 1 x 10^{-4} s^{-1} and 25°C and 480°C. Note that b) only includes the tests at 480°C so the graph can be magnified.*

At room temperature, the WHR of Ni_3Fe increased 87% with ordering. At 480°C, the WHR of the ordered alloy was still 33% higher than the disordered alloy. If APB tubes were contributing to the WHR, they would be expected to annihilate so close to the disordering temperature, and thus it is unlikely that they are responsible for the increased WHR at 480°C. *Ex-situ* TEM research has shown that the dislocation structure of ordered Ni_3Fe is still composed of superdislocations after straining at 477°C [20], so the dislocation interactions observed in TEM *in-situ* straining are likely still active and are the source of the increased WHR at both room temperature and 480°C.

(4) APB tube formation in Ni_3Al

The two main APB tube formation theories are the cross-slip annihilation mechanism [19] and the dragging mechanism [21]. In both, APB tubes are expected to align with dislocations that have a Burgers vector in the direction of the APB fault vector. In lightly deformed (<5%) Ni_3Al, APB tubes were seen connected to screw and mixed superdislocations with Burgers vectors in different directions than the APB tube fault vector, shown in **Figure 5a**. This indicates that there are either previously-unreported APB tube formation mechanisms active or that APB tubes were observed interacting with secondary dislocations. TEM *in-situ* strain testing could illuminate what mechanism is responsible for the features reported in this chapter.

One instance was observed of edge superdislocations ending at APB tubes, shown in **Figure 5b**, which is consistent with the cross-slip annihilation mechanism. This has never been reported in Ni_3Al before and bears further investigation. No evidence was seen of APB tubes dragging behind long screw superdislocations. This does not mean the dragging mechanism is not active, but the evidence presented in this chapter suggests that the dragging mechanism is not the only APB tube formation mechanism in Ni_3Al.

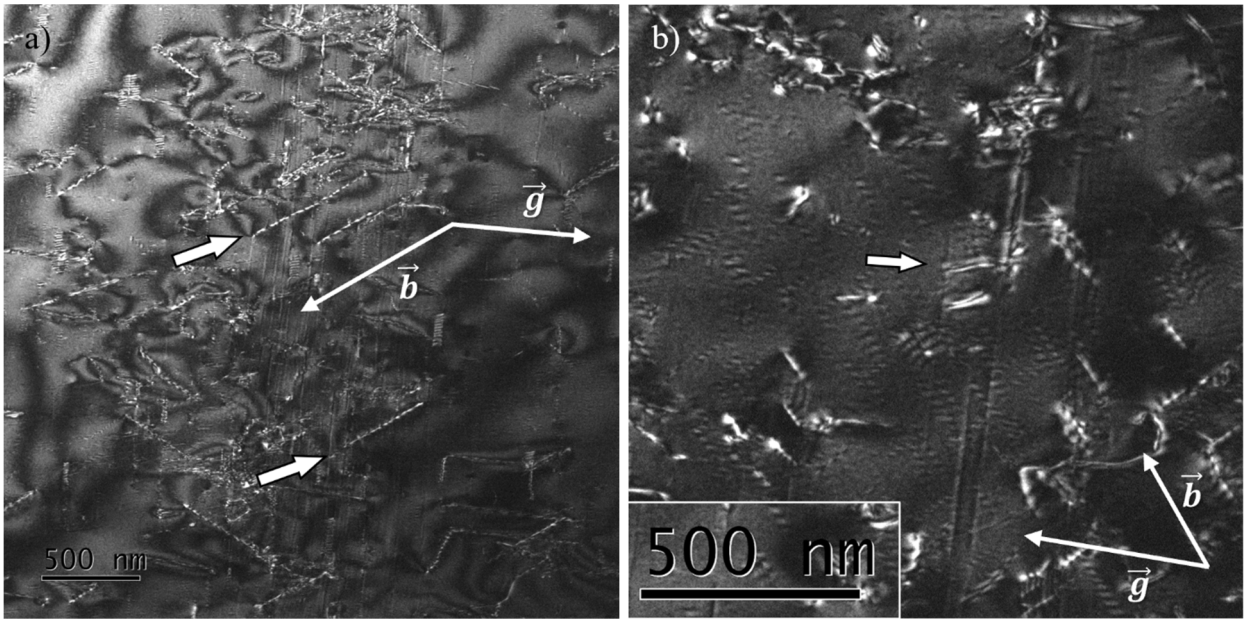

Figure 5. *TEM $\vec{g}/3\vec{g}$ WBDF images of Ni_3Al compressed 4.9% showing a) APB tubes connected to screw superdislocations (indicated with thick white arrows), imaged with $\vec{B} = [3\bar{2}5]$, $\vec{g} = [\bar{1}11]$, and $|\overrightarrow{s_g}| = 0.09\ nm^{-1}$; and edge dislocations ending at APB tubes, imaged with $\vec{B} = [119]$, $\vec{g} = [\bar{1}10]$, and $|\overrightarrow{s_g}| = 0.04\ nm^{-1}$.*

(5) Methods of quantifying APB tubes

The electrical resistivity of a single crystal of Fe-40 at.% Al was measured with a four-point collinear probe with a 30 V input voltage. The resulting values were higher than those listed in the literature [22–24]. The resistivity went from 231 ± 7 μΩ*cm to 323 ± 5 μΩ*cm after 16% reduction in thickness by cold-rolling, a 40% increase. After annealing at 120°C for 2 h (an anneal which has been shown to remove APB tubes in FeAl, but not to affect the dislocations [4–6]) the resistivity reduced to 268 ± 6 μΩ*cm and was only 16% higher than the undeformed sample. The remaining resistivity must be due to dislocations. Resistivity may work as a method of quantifying APB tubes in FeAl and bears further study. Resistivity experiments on Ni_3Fe were not conclusive.

Appendix 1: High entropy alloys (HEAs)

One of the main goals of the proposed work was to analyze the impact of APB tubes on the work hardening rate with ordering of the high entropy alloy $AlCoCrFeNi_{2.1}$. Many authors [25–27] have stated that this alloy is composed of a B2 phase and an $L1_2$ phase. However, the present authors discovered that the soft phase was actually disordered f.c.c. with coherent $L1_2$ nanoprecipitates, rather than an f.c.c. → $L1_2$ orderable alloy. At least one other group [28] has also observed this. In this case, no APB tubes could form in the alloy, and it was not suitable for the present work. FeCoNiV also seemed like a good candidate, as it has been reported to be f.c.c. → $L1_2$ orderable [27]. However, when the present authors cast FeCoNiV and observed it in the TEM there were many large precipitates that also made it unsuitable for this work. While it is certainly still possible that APB tubes form in ordered HEAs, there is no reason to think APB tubes would affect the WHR of HEAs if they do not affect the WHR of ordered binary intermetallics.

Appendix 2: Additional analysis techniques

It was theorized that the X-ray diffraction (XRD) and neutron diffraction patterns from deformed ordered intermetallics would change with the removal of APB tubes. Synchrotron XRD was performed on polycrystalline Ni_3Fe at the Cornell High Energy Synchrotron Source (CHESS). Polycrystalline Ni_3Fe was chosen because it was ductile enough to perform *in-situ* tensile testing during XRD. However, during initial testing it was discovered that the second-order harmonic of the X-rays directly overlapped the superlattice reflections of the first-order harmonic and it was not possible to fix without buying and installing a new piece of equipment on the beamline, which was not possible. This would be an issue for any of the cubic ordered intermetallics used in this project, so synchrotron XRD was not a viable technique for this project.

Neutron diffraction was performed on lightly-deformed Ni_3Fe samples at Oak Ridge National Laboratory. The superlattice peaks were discernible, which is quite difficult to achieve for Ni_3Fe. However, peak analysis was not successful to detect a difference in the peak broadening with deformation and annealing. This experiment may be worth repeating on a material where the APB tube annihilation temperature is defined, such as Fe-40 at.% Al. In Ni_3Al, it is not possible to remove only APB tubes and no other defects, and thus it would not be suitable for this work.

Personnel Supported

Ian Baker – P.I. (Partial Support)
Rachel Osmundsen – Ph.D. student (full support); PhD defended April 1st, 2022.
Ling Hu - Ph.D. Exchange student (research costs only) Oct. 2018-Jan. 2020
Hanlin Peng - Ph.D. Exchange student (research costs only), Feb. 2019 – Jan 2020
Joseph Taylor – undergraduate student (research costs only)

Publications

1. "Microband Induced Plasticity and the temperature dependence of the mechanical properties of a carbon-doped FeNiMnAlCr high entropy alloy" Z. Wang, H. Bei and I. Baker, Materials Characterization, **139** (2018) 373-381. https://doi.org/10.1016/j.matchar.2018.03.017
2. "Eutectic/Eutectoid Multi-Principle Component Alloys: A Review", I. Baker, M. Wu and Z. Wang, Materials Characterization**,** **147** (2019) 545-557. https://doi.org/10.1016/j.matchar.2018.07.030.
3. The effects of carbon on the phase stability and mechanical properties of heat-treated FeNiMnCrAl high entropy alloys, M. Wu, Z. Li, B. Gault, P. Munroe and I. Baker, Materials Science and Engineering: A, **748** (2019) 59-73. https://doi.org/10.1016/j.msea.2019.01.083
4. "Enhanced Mechanical Properties of Carbon-doped FeNiMnAlCr High Entropy Alloy via Hot-Rolling", M. Wu, C. Yang, M. Kuijer and I. Baker, Materials Characterization, 158 (2019) 109983 (6 pages). https://doi.org/10.1016/j.matchar.2019.109983.
5. "Characterization of high-strength high-nitrogen austenitic stainless steel synthesized from nitrided powders by spark plasma sintering", L. Hu, H. Peng, L. Lia, Ian Baker, W. Zhang, Materials Characterization, 152 (2019) 76-84. https://doi.org/10.1016/j.matchar.2019.04.005.
6. "High Strength and High Ductility in a Novel $Fe_{40.2}Ni_{11.3}Mn_{30}Al_{7.5}Cr_{11}$ Multiphase High Entropy Alloy", M. Wu and I. Baker, Journal of Alloys and Compounds, 820 (2020) 153181 (11 pages). https://doi.org/10.1016/j.jallcom.2019.153181.
7. "High Strength and High Ductility in a Novel $Fe_{40.2}Ni_{11.3}Mn_{30}Al_{7.5}Cr_{11}$ Multiphase High Entropy Alloy", M. Wu and I. Baker, Journal of Alloys and Compounds, 820 (2020) 153181 (11 pages). https://doi.org/10.1016/j.jallcom.2019.153181.
8. "Interstitials in f.c.c. High Entropy Alloys", I. Baker, Metals, **10** (2020) 695 (20 pages). doi:10.3390/met10050695
9. "The effect of antiphase boundary tubes on the hardness of FeAl," R. Osmundsen and I. Baker, Metallurgical and Materials Transactions A, **52** (2021), 3694-3698. https://doi.org/10.1007/s11661-021-06355-w
10. "Optimization of the microstructure and mechanical properties of electron beam welded high-strength medium-entropy alloy $(NiCoCr)_{94}Al_3Ti_3$", Hanlin Peng, Yaoyong Yi, Weiping Fang, Ling Hu, Ian Baker, Liejun Li and Bingbing Luo, Intermetallics, **141** (2022) 107439. https://doi.org/10.1016/j.intermet.2021.107439
11. "New insights on the work hardening mechanisms of ordered alloys with special attention to antiphase boundary tubes". Rachel Osmundsen, PhD. Thesis, Dartmouth College, April 2022.
12. "Interstitial Strengthening in f.c.c. Metals and Alloys", I. Baker, Advanced Powder Materials, **1** (2022) 100034. https://doi.org/10.1016/j.apmate.2022.100034

Papers Submitted for Publication

1. "The annihilation of antiphase boundary tubes and their effect on strengthening in Ni_3Al," Rachel Osmundsen and Ian Baker, *under review* at Acta Materialia
2. "Simultaneous twinning and microband-induced plasticity of a compositionally complex alloy with interstitial Carbon at cryogenic temperatures," A. S. Tirunilai, R. Osmundsen, I. Baker,

H. Chen, K.-P. Weiss, M. Heilmaier, A. Kauffman, *under review* at High Entropy Alloys & Materials

Papers in Preparation

1. "Study of the strengthening mechanisms of ordered and disordered Ni_3Fe by TEM *in-situ* straining and bulk tensile testing," Rachel Osmundsen and Ian Baker.

Patent

United States Patent 1,0190,197 "Oxidation Resistant High-Entropy Alloys", 1/29/19, Ian Baker and Zhangwei Wang.

Invited Presentations

1. "Designing Low-Cost, High Strength, Ductile, High Entropy, Stainless Steels", I. Baker, THERMEC'2018 International Conference on Processing and Manufacturing of Advanced Materials: Processing, Fabrication, Properties, Applications, *July 8-13, 2018, Paris, France.*
2. "Strain-Induced Ferromagnetism in Intermetallic Compounds", I. Baker, 5th International Conference on Materials Science and Smart Materials "MSSM 2018", Glasgow, United Kingdom, 7-11 August, 2018. (KEYNOTE SPEAKER)
3. "APB tubes in intermetallic compounds", I. Baker, Gordon Research Conference on Structural Nanomaterials, The Hong Kong University of Science and Technology, Hong Kong, China, 12-17 August , 2018.
4. "Engineering New Materials for the Future", I. Baker, Museum of the Rockies, Bozeman, Montana, September 18th, 2019.
5. "Designing Low-Cost, High Strength, Ductile, High Entropy, Stainless Steels", I. Baker, Lehigh University, Bethlehem, Pa, November 1st, 2019.
6. "High entropy FeNiMnAlCr alloys", I. Baker, Institut NÉEL, CNRS/UGA, Grenoble, France, December 18th, 2019.
7. "The roles of Anti-phase boundary tubes on magnetic and mechanical properties of intermetallic compounds", I. Baker, Institut NÉEL, CNRS/UGA, Grenoble, France, December 18th, 2019.
8. "High Entropy FeNiMnAlCr alloys", I. Baker, Ciclo de seminaries virtuales: Materiales estructurales, Materials Research Institute (IIM) of the National Autonomous University of Mexico (UNAM), Mexico, October 8th, 2020.
9. "The Roles of Anti-phase Boundary Tubes on Magnetic and Mechanical Properties of Intermetallic Compounds", I. Baker, GSO Mini-Speaker series, U. New Hampshire May 5, 2021.
10. "FeNiMnAlCr Multi-Principal Component Alloys", I. Baker, Johns Hopkins University, February 8th, 2022.

Other Presentations (* indicates speaker)

1. "The Microstructure and Mechanical Properties of High Strength, Ductile, Eutectic FeNiMnAl(Cr,Ti) High-Entropy Alloys", I. Baker*, Z. Wang, M. Wu and F. Meng, Materials Science & Technology Conference & Exhibition – MS & T 2018, Columbus, OH, October 14-18.

2. “Thermo-mechanical Processing of Carbon-doped FeNiMnAlCr High Entropy Alloys”, M. Wu* and I. Baker, Materials Science & Technology Conference & Exhibition - MS&T 2018, Columbus, OH, October 14-18.
3. “FeMnNiAlCr High Entropy Alloys (HEAs) and Their Native Oxide Solar Absorbers for Concentrated Solar Power Systems” E. Lee*, M. Wu, S. Somers, I. Baker and J. Liu, Symposium on Intermetallics - from Fundamentals to Applications, Materials Research Society meeting, Boston, MA, 27 Nov. – 1 Dec., 2018.
4. “Quantifying the Role of APB Tubes on the Work-hardening of Ordered Phases”, Ian Baker and Rachel Osmundsen*, poster at DOE Contractors meeting, Gaitherberg, MD, August 13-15, 2019.
5. “Deformation Microstructure of an $L1_2$ Intermetallic High Entropy Alloy,” Rachel Osmundsen* and Ian Baker, MRS Fall 2020, November 24-December 4, 2020.
6. “Deformation behavior of a single phase $L1_2$ Intermetallic High Entropy Alloy,” Rachel Osmundsen* and Ian Baker, Thermec’2021 International Conference on Processing & Manufacturing of Advanced Materials, May 10-14, 2021.

Collaborators

Dr. Si Chen - Argonne National Laboratory, performed synchrotron X-ray diffraction
Dr. Katherine Shanks – Cornell High Energy Synchrotron Source (CHESS), performed synchrotron X-ray diffraction and assisted with data analysis
Dr. Kelly Nygren – CHESS, performed synchrotron X-ray diffraction and assisted with data analysis

Acknowledgements

This research used resources at the Spallation Neutron Source, a DOE Office of Science User Facility operated by the Oak Ridge National Laboratory. Special thanks to Dr. Qiang Zhang for support designing the experiments.

This research used resources at the Cornell High Energy Synchrotron Source. Special thanks to Dr. Katherine Sato Shanks and Dr. Kelly Nygren for supporting this remote experiment.

Works Cited

[1] A.E. Vidoz, L.M. Brown, On work-hardening in ordered alloys, Philos. Mag. 7 (1962) 1167–1175. https://doi.org/10.1080/14786436208209116.
[2] C.T. Chou, P.B. Hirsch, Antiphase domain boundary tubes in plastically deformed ordered Fe 30.5 at.% Al alloy, Philos. Mag. A. 44 (1981) 1415–1419. https://doi.org/10.1080/01418618108235822.
[3] P.M. Hazzledine, Y.Q. Sun, The strain field and work-hardening from antiphase boundary tubes in ordered alloys, Mater. Sci. Eng. A. 152 (1992) 189–194. https://doi.org/10.1016/0921-5093(92)90066-A.
[4] D. Wu, I. Baker, The activation energies of antiphase-boundary tube annihilation in Fe-Al, Philos. Mag. 82 (2002) 2239–2247. https://doi.org/https://doi.org/10.1080/01418610208235735.
[5] D. Wu, P.R. Munroe, I. Baker, The paramagnetic-to-ferromagnetic transition in B2-structured Fe-Al single crystals: Experiments and calculations, Philos. Mag. 83 (2003) 295–313.

https://doi.org/10.1080/0141861021000042280org/10.1080/0141861021000042280.
[6] Y. Yang, I. Baker, P. Martin, On the mechanism of the paramagnetic-to-ferromagnetic transition in Fe-Al, Philos. Mag. B. 79 (1999) 449–461. https://doi.org/10.1080/13642819908206419.
[7] Y. Yang, I. Baker, Annealing of quenched Fe-Al alloys with/without B and Ti, Mater. Res. Soc. Symp. - Proc. 552 (1999) 1–5. https://doi.org/10.1557/proc-552-kk8.22.1.
[8] A.H.W. Ngan, A simple string model for annihilation of antiphase-boundary tubes in intermetallic compounds, Philos. Mag. A. 71 (1995) 725–734. https://doi.org/10.1080/01418619508244478.
[9] P.M. Hazzledine, P. Hirsch, Antiphase domain boundary tubes in ordered alloys, Mat. Res. Soc. Symp. Proc. 81 (1987) 75–85. https://doi.org/10.1557/PROC-81-75.
[10] F.X. Kayser, C. Stassis, The elastic constants of Ni3Al at 0 and 23.5 °C, Phys. Status Solidi. 64 (1981) 335–342. https://doi.org/10.1002/pssa.2210640136.
[11] K.J. Hemker, M.J. Mills, Measurements of antiphase boundary and complex stacking fault energies in binary and B-doped Ni_3Al using TEM, Philos. Mag. A. 68 (1993) 305–324. https://doi.org/10.1080/01418619308221207.
[12] S. Ghosh Chowdhury, A.K. Jena, R.K. Ray, Recovery and ordering in cold-rolled boron-doped $Ni_{76}Al_{24}$, Metall. Mater. Trans. A. 31 (2000) 2127–2134. https://doi.org/10.1007/s11661-000-0130-2.
[13] H.P. Karnthaler, R. Kozubski, W. Pfeiler, C. Rentenberger, Defect recovery and ordering in Ni_3Al+B, Mat. Res. Soc. Symp. Proc. 364 (1995) 309–314. https://doi.org/https://doi.org/10.1557/PROC-364-309.
[14] S.S. Ezz, P.B. Hirsch, The strain rate sensitivity of the flow stress and the mechanism of deformation of single crystals of Ni_3(Al Hf)B, Philos. Mag. A. 69 (1994) 105–127. https://doi.org/10.1080/01418619408242213.
[15] T. Kruml, J.L. Martin, B. Viguier, J. Bonneville, P. Spätig, Deformation microstructures in Ni_3(Al, Hf), Mater. Sci. Eng. A. 239–240 (1997) 174–179. https://doi.org/10.1016/s0921-5093(97)00578-9.
[16] P.H. Thornton, R.G. Davies, T.L. Johnston, The temperature dependence of the flow stress of the γ′ phase based upon Ni_3Al, Metall. Trans. 1 (1970) 207–218. https://doi.org/10.1007/BF02819263.
[17] T. Kruml, E. Conforto, B. Lo Piccolo, D. Caillard, J.L. Martin, From dislocation cores to strength and work-hardening: A study of binary Ni_3Al, Acta Mater. 50 (2002) 5091–5101. https://doi.org/10.1016/S1359-6454(02)00364-6.
[18] A.E. Staton-Bevan, The orientation and temperature dependence of the work-hardening rate of single crystal Ni_3(Al, Ti), Philos. Mag. A. 47 (1983) 939–949. https://doi.org/10.1080/01418618308243131.
[19] R.J. Wakelin, E.L. Yates, A Study of the Order-Disorder Transformation in Iron-Nickel Alloys in the Region $FeNi_3$, Proceeding Phys. Soc. Sect. B. 66 (1953) 221–240. https://doi.org/10.1088/0370-1301/66/3/310.
[20] A. Korner, Mechanical properties and dislocation structure in $L1_2$ long-range ordered Ni_3Fe, Philos. Mag. Lett. 63 (1991) 117–122. https://doi.org/10.1080/09500839108205979.
[21] X. Shi, G. Saada, P. Veyssière, The formation of antiphase-boundary tubes in Ni_3Al, Philos. Mag. A. 73 (1996) 1159–1171. https://doi.org/10.1080/01418619608243711org/10.1080/01418619608243711.

[22] B. V. Reddy, S.C. Deevi, Thermophysical properties of FeAl (Fe-40 at.%Al), Intermetallics. 8 (2000) 1369–1376. https://doi.org/10.1016/S0966-9795(00)00084-4.
[23] M. Kass, C.R. Brooks, D. Falcon, D. Basak, The formation of defects in Fe-Al alloys: electrical resistivity and specific heat measurements, Intermetallics. 10 (2002) 951–966. https://doi.org/10.1016/S0966-9795(02)00115-2.
[24] A. Pazourek, W. Pfeiler, V. Šíma, Dependence of electrical resistivity of Fe-Al alloys on composition, Intermetallics. 18 (2010) 1303–1305. https://doi.org/10.1016/j.intermet.2010.01.019.
[25] I.S. Wani, T. Bhattacharjee, S. Sheikh, P.P. Bhattacharjee, S. Guo, N. Tsuji, Tailoring nanostructures and mechanical properties of $AlCoCrFeNi_{2.1}$ eutectic high entropy alloy using thermo-mechanical processing, Mater. Sci. Eng. A. 675 (2016) 99–109. https://doi.org/10.1016/j.msea.2016.08.048.
[26] Q. Wang, Y. Lu, Q. Yu, Z. Zhang, The Exceptional Strong Face-centered Cubic Phase and Semi-coherent Phase Boundary in a Eutectic Dual-phase High Entropy Alloy AlCoCrFeNi, Sci. Rep. 8 (2018) 1–7. https://doi.org/10.1038/s41598-018-33330-0.
[27] N.R. Jaladurgam, A. Lozinko, S. Guo, T.L. Lee, M.H. Colliander, Temperature dependent load partitioning and slip mode transition in a eutectic $AlCoCrFeNi_{2.1}$ high entropy alloy, Materialia. (2021). https://doi.org/https://doi.org/10.1016/j.electacta.2021.138466.
[28] T. Xiong, S. Zheng, J. Pang, X. Ma, High-strength and high-ductility $AlCoCrFeNi_{2.1}$ eutectic high-entropy alloy achieved via precipitation strengthening in a heterogeneous structure, Scr. Mater. 186 (2020) 336–340. https://doi.org/10.1016/j.scriptamat.2020.04.035.